

Decoupled Trajectory Tracking Controllers Design for Multirotors

Hao LIU

School of Astronautics, Beihang University, P. R. China
liuhao13@buaa.edu.cn

Jonghyuk KIM

Research School of Engineering, Australian National University, Australia
jonghyuk.kim@anu.edu.au

Abstract

A controller design method is proposed to control quadrotors with six degrees of freedom. The vehicle system is divided into four subsystems: the longitudinal, lateral, yaw, and height subsystems. A linear and decoupled nominal model is obtained for each subsystem, while coupling and nonlinear dynamics, parametric perturbations, and external disturbances are considered as uncertainties. For each subsystem, a decoupled robust controller is proposed. Although there exist couplings between each channel, the output tracking errors of the four subsystems are proven to ultimately converge into *a-priori* set neighborhood of the origin. Real-time implementation results of the decoupled controller are given to demonstrate its viability.

1 Introduction

In the two decades, there has been an increasing interest in unmanned helicopters for various applications as shown in [Gadewadikar *et al.*, 2009; Liu *et al.*, 2012; Godbolt *et al.*, 2013; Raptis *et al.*, 2011]. The helicopters have several advantages over the fixed wing aircrafts as shown in [Das *et al.*, 2009].

Compared to conventional helicopters, multirotor aircrafts are more maneuverable and have simpler mechanism, thus attracting more interests. The quadrotor, which possesses four rotors and is shown in Fig.1, is regarded as one kind of typical multirotor aircrafts and extensive studies have been made to achieve their automatic flight. The quadrotor is a nonlinear dynamic system with six degrees of freedom (6 DOF). Full dynamic system incorporating 6 DOF was considered in [Hamel and Mahony, 2002], and a Lyapunov-based control algorithm was derived based on the backstepping techniques for a small model autonomous helicopter to stabilize over a marked landing pad. In [Das *et al.*, 2004], a dynamic model of the quadrotor was obtained by applying the Lagrange modeling method, and a nested saturation control was used for the quadrotor to perform autonomous missions of taking-off and landing vertically. A two-camera method was introduced to estimate the pose information in [Altug *et al.*, 2005], and a controller using the feedback linearization and backstepping-based approach was proposed for the quadrotor. In [Hoffmann *et al.*, 2011] and [Pounds *et al.*, 2010], the classic proportional-integral-derivative (PID) controller was investigated to control a quadrotor robot. A partial state feedback control law was designed via the singular perturbation theory for a miniature quadrotor UAV as shown in [Bertrand *et al.*, 2011]. How-



Figure 1: The quadrotor in hover.

ever, generally, the quadrotor system is subject to various uncertainties such as parameter perturbations, unmodeled uncertainties, and external disturbances. Therefore, recently, research has been focused extensively on robust control of quadrotors (see, e.g. [Zuo, 2010; Zhang *et al.*, 2011; Guerrero-Castellanos *et al.*, 2011; Zhong, 2002]). However, many of these works have addressed uncertainties involved in the rotational dynamics of the quadrotors, whereas designing robust controllers against the uncertainties in the full 6-DOF dynamics of these vehicles is still challenging.

In the current paper, the robust position control problem of the quadrotor is investigated. The influence of uncertainties existing in the 6-DOF motion of the vehicle is required to be restrained. Instead of directly dealing with the full nonlinearity, a robust and quite practical decoupled approach is proposed. The quadrotor system is firstly divided into four subsystems: the height subsystem, the longitudinal subsystem, the lateral subsystem, and the yaw subsystem. A linear and decoupled nominal model is then obtained through a system identification for each subsystem, and all uncertainties are included as the equivalent disturbances. Finally, a linear time-invariant and robust controller is proposed for each subsystem. Compared to the existing works on quadrotor control, the uncertainties involved in the 6-DOF dynamics can be restrained. Second, although there exists coupling between each subsystem, a decoupled control is achieved for the quadrotor. In addition, the resulted controller has a form of linear time-invariant and decoupled structure, which is easy

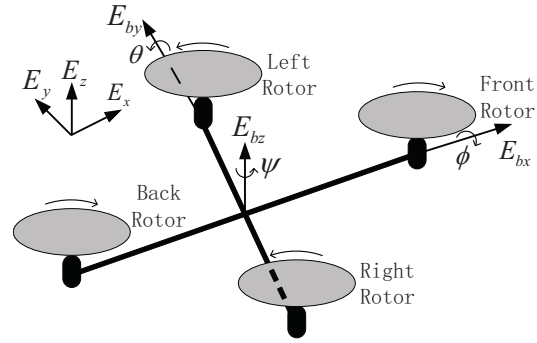


Figure 2: Schematic of quadrotor.

to implement in practical applications.

2 Model Description

In this section, the inertial frame and the body fixed frame are introduced. Let $E = \{E_x, E_y, E_z\}$ denote the inertial frame, which is considered fixed to the Earth. As depicted in Fig.2, let $E_b = \{E_{bx}, E_{by}, E_{bz}\}$ be the body fixed frame linked to the quadrotor, which is considered as a rigid body. The origin of the body fixed frame is the mass center of the vehicle. Denote $\xi = [\xi_x \ \xi_y \ \xi_z]^T$ the position of the vehicle expressed in the frame E and $\eta = [\phi \ \theta \ \psi]^T$ the three Euler angles, which determine the quadrotor orientation from E to E_b [Zhong, 2002]. ϕ is the roll angle, θ the pitch angle, and ψ the yaw angle as shown in Fig.2. The quadrotor has four rotors: the front rotor, the back rotor, the left rotor, and the right rotor. By changing the lift forces produced by the four rotors, the quadrotor can achieve various maneuvers. The vertical motion can be achieved by changing the total thrust generated by the four rotors. The quadrotor has four control inputs $u_i (i = 1, 2, 3, 4)$ to change the external torques around the axes E_{by} , E_{bx} , and E_{bz} and the total lift force produced by the four rotors respectively.

The quadrotor system thus consists of four subsystems: the longitudinal subsystem, the lateral subsystem, the yaw subsystem, and the

height (vertical) subsystem. Corresponding inputs and outputs for the four subsystems are u_1 and ξ_x , u_2 and ξ_y , u_3 and ψ , and u_4 and ξ_z , respectively. The dynamics of the longitudinal and lateral subsystems are modeled as the following systems:

$$\begin{aligned}\ddot{\xi}_x &= a_{0x}\xi_x + a_{1x}\dot{\xi}_x + b_{1x}\theta, \\ \ddot{\theta} &= a_{2x}\theta + a_{3x}\dot{\theta} + b_{2x}u_1, \\ \ddot{\xi}_y &= a_{0y}\xi_y + a_{1y}\dot{\xi}_y + b_{1y}\phi, \\ \ddot{\phi} &= a_{2y}\phi + a_{3y}\dot{\phi} + b_{2y}u_2,\end{aligned}\quad (1)$$

and the yaw and height subsystems as

$$\begin{aligned}\ddot{\psi} &= a_{0\psi}\psi + a_{1\psi}\dot{\psi} + b_\psi u_3, \\ \ddot{\xi}_z &= a_{0z}\xi_z + a_{1z}\dot{\xi}_z + b_z u_4,\end{aligned}\quad (2)$$

where a_i and b_i are nominal parameters determined from the system identification. From (1) and (2), one can see that for each subsystem, only a linear time-invariant and single-input single-output (SISO) model is required, which can be obtained easily.

Let $r_i (i = x, y, \psi, z)$ be the desired references for ξ_x , ξ_y , ψ , and ξ_z respectively. Then the models can be rewritten in terms of error variables which are defined as $e_x = [e_{x,j}]_{4 \times 1}$, $e_y = [e_{y,j}]_{4 \times 1}$, $e_\psi = [e_{\psi,j}]_{2 \times 1}$, and $e_z = [e_{z,j}]_{2 \times 1}$, where $e_{i,1} = \xi_i - r_i (i = x, y, z)$, $e_{\psi,1} = \psi - r_\psi$, $e_{x,3} = \theta + (a_{0x}r_x + a_{1x}\dot{r}_x - \ddot{r}_x)/b_x$, $e_{y,3} = \phi + (a_{0y}r_y + a_{1y}\dot{r}_y - \ddot{r}_y)/b_y$, $e_{i,j} = \dot{e}_{i,j-1} (i = x, y; j = 2, 4)$, and $e_{k,2} = \dot{e}_{k,1} (k = \psi, z)$. Let

$$A_i = \begin{bmatrix} 0 & 1 & 0 & 0 \\ a_{0i} & a_{1i} & b_{1i} & 0 \\ 0 & 0 & 0 & 1 \\ 0 & 0 & a_{2i} & a_{3i} \end{bmatrix}, B_i = \begin{bmatrix} 0 \\ 0 \\ 0 \\ b_{2i} \end{bmatrix}, \quad i = x, y, \quad (3)$$

and

$$A_j = \begin{bmatrix} 0 & 1 \\ a_{0j} & a_{1j} \end{bmatrix}, B_j = \begin{bmatrix} 0 \\ b_j \end{bmatrix}, j = \psi, z.$$

Then, the error dynamic model for a single subsystem becomes

$$\dot{e}_i = A_i e_i + B_i (u_i + \Delta_i), i = x, y, \psi, z, \quad (4)$$

where $\Delta_i (i = \theta, \phi, \psi, z)$ are the named equivalent disturbances which involve uncertainties such as coupling and nonlinear dynamics, parametric perturbations, and external disturbances.

By combining all subsystems, one can see that the whole quadrotor error system in a matrix-vector form can be described as

$$\dot{e} = Ae + B(u + \Delta), \quad (5)$$

where $e = [e_x^T \ e_y^T \ e_\psi^T \ e_z^T]^T$, $u = [u_x \ u_y \ u_\psi \ u_z]^T$, $\Delta = [\Delta_x \ \Delta_y \ \Delta_\psi \ \Delta_z]^T$, and

$$\begin{aligned}A &= \text{diag}(A_x, A_y, A_\psi, A_z), \\ B &= \text{diag}(B_x, B_y, B_\psi, B_z).\end{aligned}$$

Assumption 1 For the equivalent disturbances $\Delta_i (i = 1, 2, 3, 4)$, there exist positive constants ς_{ei} , $\delta_i < 1$, and ς_{ci} such that $\|\Delta_i\|_\infty \leq \varsigma_{ei}\|e\|_\infty + \delta_i\|u_i\|_\infty + \varsigma_{ci}$.

This assumption means that the equivalent disturbances are norm bounded. This is a reasonable assumption in many practical systems.

3 Decoupled Controller Design

In this paper, the goal of the designed controller is to achieve the desired tracking properties of the closed-loop control system: for *a-priori* set constants ε and a given bounded initial state $e(0)$, there exists a positive constant T , such that the state of the whole quadrotor system is bounded and satisfies that $|e(t)| \leq \varepsilon, \forall t \geq T$.

If the uncertainties Δ is ignored, the error model (5) is the nominal model. The control inputs $u_i (i = x, y, \psi, z)$ consists of two parts: the nominal part $u_i^N (i = x, y, \psi, z)$ and the robust compensating part $u_i^R (i = x, y, \psi, z)$ as

$$u_i = u_i^N + u_i^R, i = x, y, \psi, z. \quad (6)$$

The nominal inputs are designed for each nominal system to achieve the desired tracking, while the robust compensating inputs are introduced to restrain the effects of the uncertainties Δ .

The nominal feedback control laws for the four subsystems are designed based on the static feedback control approach as follows

$$u_i^N = -K_i e_i, i = x, y, \psi, z. \quad (7)$$

Denote $A_{iH} = A_i - B_i K_i (i = x, y, \psi, z)$, where the parameters of the matrix K_i are selected such that A_{iH} is Hurwitz. Then the closed-loop system dynamics becomes

$$\dot{e}_i = A_{iH} e_i + B_i (u_i^R + \Delta_i), i = x, y, \psi, z. \quad (8)$$

The robust compensating inputs $u_i^R (i = x, y, \psi, z)$ are to be designed to restrain the effects of the equivalent disturbances Δ_i , such that the closed-loop control system could respond as the nominal system $\dot{e}_i = A_{iH} e_i$. However, $\Delta_i (i = x, y, \psi, z)$ cannot be measured directly, and therefore robust filters are introduced (see also in [Liu *et al.*, 2013]). The robust filters have the following forms

$$\begin{aligned} F_i(p) &= f_i^4 / (f_i + p)^4, i = x, y, \\ F_j(p) &= f_j^2 / (f_j + p)^2, j = \psi, z, \end{aligned} \quad (9)$$

where p is the Laplace operator and $f_i (i = x, y, \psi, z)$ are positive constants. If $f_i (i = x, y, \psi, z)$ are sufficiently large, one can expect that these robust filters have sufficiently wide frequency bandwidths and thereby the gains of the filters would approximate to 1. The compensator control outputs are chosen as the lowpass-filtered disturbances as

$$u_i^R(p) = -F_i(p) \Delta_i(p), i = x, y, \psi, z. \quad (10)$$

From (4) and (10), one can obtain the following state-space realization of the robust compensating input in the yaw subsystem

$$\begin{aligned} \dot{z}_{\psi 1} &= -f_{\psi} z_{\psi 1} - (f_{\psi}^2 + a_{1\psi} f_{\psi} - a_{0\psi}) e_{\psi, 1} \\ &\quad + b_{\psi} u_{\psi}, \\ \dot{z}_{\psi 2} &= -f_{\psi} z_{\psi 2} + (2f_{\psi} - a_{1\psi}) e_{\psi, 1} + z_{\psi 1}, \\ u_{\psi}^R &= f_{\psi}^2 (z_{\psi 2} - e_{\psi, 1}) / b_{\psi}. \end{aligned} \quad (11)$$

From the above equations, one can see that the robust compensating input u_{ψ}^R does not depend on the uncertainties Δ_{ψ} . The realization

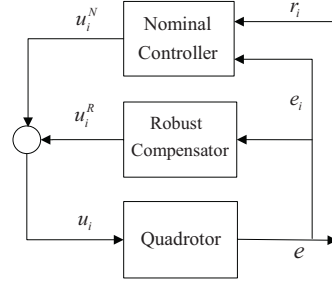


Figure 3: The schematic diagram of the closed-loop robust control system. It consists of four subsystems: the longitudinal subsystem ($i = x$), the lateral subsystem ($i = y$), the yaw subsystem ($i = \psi$), and the height subsystem ($i = z$).

of the robust compensating inputs in other subsystems can be achieved in similar ways. The whole schematic diagram of the robust and decoupled control system is depicted in Fig.3.

From (7) and (11), one can see that, actually, a decoupled control is achieved for the four subsystems. Furthermore, the resulted controller is a linear time-invariant one, which is easily implementable in practical applications.

4 Robustness Property Analysis

In this section, the robust tracking properties of the whole closed-loop control system are analyzed.

Theorem 1: If the assumption presented in the second section can be met, then, for *a-priori* set constant $\varepsilon > 0$ and bounded initial state, there exist a constant $T > 0$ and parameters $f_i > 0 (i = x, y, \psi, z)$ with sufficiently large values, such that e is bounded and $|e(t)| \leq \varepsilon, \forall t \geq T$.

This theorem can be proven based on the small gain theory.

5 Real-time Implementation of Decoupled Controller

Using the quadrotor systems as shown in Fig.1, real-time position control is experimented. The

Table 1: HELICOPTER PARAMETERS

Parameter	Value	Parameter	Value
a_{0x}	0	a_{1x}	0
a_{2x}	0	a_{3x}	0
a_{0y}	0	a_{1y}	0
a_{2y}	0	a_{3y}	0
$a_{0\psi}$	0	$a_{1\psi}$	0
a_{0z}	0	a_{1z}	0
b_{1x}	9.81	b_{2x}	9.7
b_{1y}	9.81	b_{2y}	9.2
b_{ψ}	9.81	b_z	9.81

nominal values of the helicopter parameters are shown as in Table 1. Moreover, the nominal controller parameters are chosen as: $K_x = [1 \ 3 \ 6 \ 2]$, $K_y = [1 \ 3 \ 6 \ 2]$, $K_\psi = [5 \ 3]$, and $K_z = [2.5 \ 45]$ by trial and error. The robust compensator parameters for each subsystem are selected as: $f_x = 1$, $f_y = 1$, $f_\psi = 1$, and $f_z = 1$ by tuning on-line.

5.1 Case 1: Step responses

Then, the proposed closed-loop system is evaluated by step tracking missions. The longitudinal position is firstly needed to follow a step signal with the amplitude of 2 m, whereas the lateral and height positions are required to be stabilized at 0 m and 0.5 m respectively. Then, the lateral position is also required to track this signal and longitudinal and height positions are required to be stabilized at 0 m and 0.5 m respectively. Responses are shown in Fig.4 and Fig.5, respectively. From the figures, it can be observed that desired step responses were tracked robustly and consistently by the proposed decoupled control method.

5.2 Case 2: Trajectory tracking

In this case, the quadrotor is required to follow a horizontal circle with a radius of 1 m. The references of the height position and the yaw angle are set to be 1 m and 0 deg, respectively. Corresponding position responses and attitude

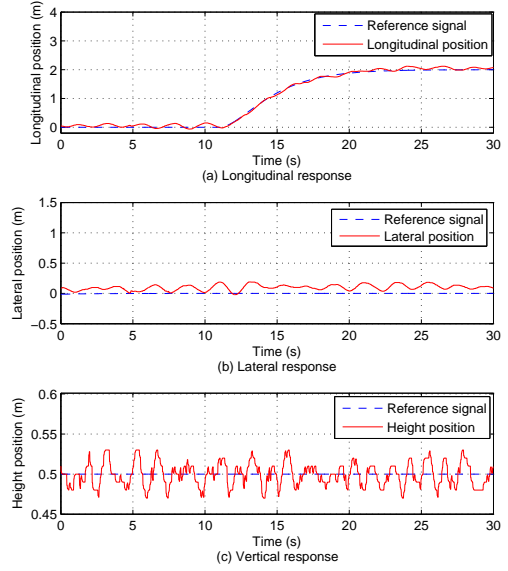


Figure 4: Step responses for the longitudinal position.

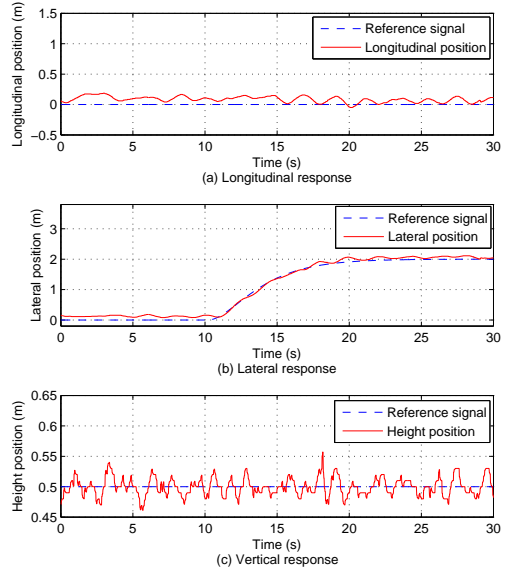


Figure 5: Step responses for the lateral position.

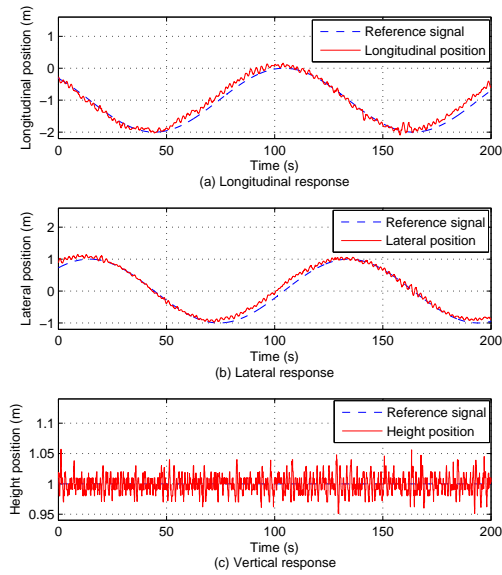


Figure 6: Responses of the three positions.

angle responses are presented in Fig.6 and Fig.7 respectively. Good automatic flight results have been achieved.

6 Conclusions

A robust and decoupled controller was proposed for a six degrees of freedom quadrotor to achieve the automatic hovering and trajectory following. The quadrotor system was divided into four subsystems and a robust controller including a nominal controller and a robust compensator was designed for each subsystem. Theoretical analysis was provided showing the convergence property of the closed-loop system and real-time experimental results demonstrate the viability and applicability of the proposed decoupled controller. Currently this method is being applied to more general multicopter models and tested under outdoor environments where wind disturbances are more severe.

Acknowledgement This work was supported by the National Natural Science Foundation of China under Grants 61503012, 61374054,

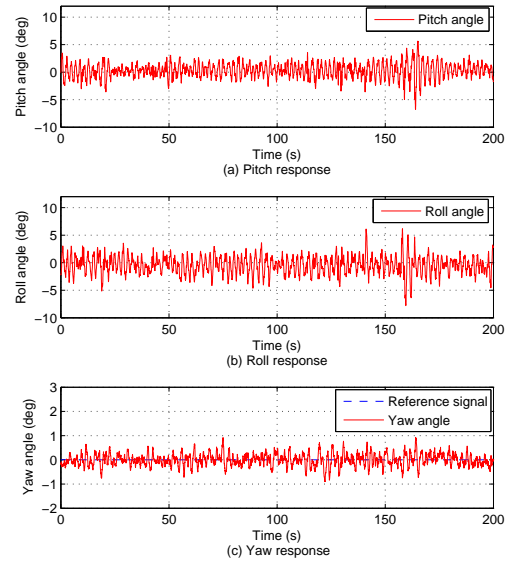


Figure 7: Responses of the three Euler angles.

61473324, 61210012, and 61263002.

References

- [Altug *et al.*, 2005] E. Altug, J. P. Taylor, and C. J. Taylor. Control of a quadrotor helicopter using dual camera visual feedback. *International Journal of Robotics Research*, 24(5):329–341, May 2005.
- [Bertrand *et al.*, 2011] S. Bertrand, N. Guegnard, T. Hamel, H. Piet-Lahanier, and L. Eck. A hierarchical controller for miniature VTOL UAVs: design and stability analysis using singular perturbation theory. *Control Engineering Practice*, 19(10):1099–1108, October 2011.
- [Das *et al.*, 2004] P. Castillo, A. Dzul, and R. Lozano. Real-time stabilization and tracking of a four-rotor mini rotorcraft. *IEEE Transactions on Control Systems Technology*, 12(4):510–516, July 2004.
- [Das *et al.*, 2009] A. Das, F. Lewis, and K. Subbarao. Backstepping approach for controlling

- a quadrotor using Lagrange form dynamics. *Journal of Intelligent and Robotic Systems*, 56(1-2):127–151, September 2009.
- [Gadewadikar *et al.*, 2009] J. Gadewadikar, F. L. Lewis, K. Subbarao, K. Peng, and B. M. Chen. H-infinity static output-feedback control for rotorcraft. *Journal of Intelligent and Robotic Systems*, 54(4):629–646, April 2009.
- [Godbolt *et al.*, 2013] B. Godbolt, N. I. Vitzilaios, and A. F. Lynch. Experimental validation of a helicopter autopilot design using model-based PID control. *Journal of Intelligent and Robotic Systems*, 70(1-4):385–399, April 2013.
- [Guerrero-Castellanos *et al.*, 2011] J. F. Guerrero-Castellanos, N. Marchand, A. Hably, S. Lesecq, and J. Delamare. Bounded attitude control of rigid bodies: real-time experimentation to a quadrotor mini-helicopter. *Control Engineering Practice*, 19(8):790–797, August 2011.
- [Hamel and Mahony, 2002] T. Hamel and R. Mahony. Visual servoing of an under-actuated dynamic rigid-body system: an image-based approach. *IEEE Transactions on Robotics and Automation*, 18(2):187–198, April 2002.
- [Hoffmann *et al.*, 2011] G. M. Hoffmann, H. Huang, S. L. Waslander, and C. J. Tomlin. Precision flight control for a multi-vehicle quadrotor helicopter testbed. *Control Engineering Practice*, 19(9):1023–1036, September 2011.
- [Liu *et al.*, 2012] C. Liu, W. Chen, and J. Andrews. Tracking control of small-scale helicopters using explicit nonlinear MPC augmented with disturbance observers. *Control Engineering Practice*, 20(3):258–268, March 2012.
- [Liu *et al.*, 2013] H. Liu, G. Lu, and Y. Zhong. Robust LQR attitude control of a 3-DOF lab helicopter for aggressive maneuvers. *IEEE Transactions on Industrial Electronics*, 60(10):4627–4636, October 2013.
- [Liu *et al.*, 2015] H. Liu, X. Wang, and Y. Zhong. Quaternion-based robust attitude control for uncertain robotic quadrotors. *IEEE Transactions on Industrial Informatics*, 11(2):406–415, April 2015.
- [Pounds *et al.*, 2010] P. Pounds, R. Mahony, and P. Corke. Modelling and control of a large quadrotor robot. *Control Engineering Practice*, 18(7):691–699, July 2010.
- [Raptis *et al.*, 2011] I. A. Raptis, K. P. Valavanis, and W. A. Moreno. A novel nonlinear backstepping controller design for helicopters using the rotation matrix. *IEEE Transactions on Control Systems Technology*, 19(2):465–473, March 2011.
- [Zhang *et al.*, 2011] R. Zhang, Q. Quan, and K.-Y. Cai. Attitude control of aquadrotor aircraft subject to a class of time-varying disturbances. *IET Control Theory and Application*, 5(9):1140–1146, June 2011.
- [Zhong, 2002] Y. Zhong. Robust output tracking control of SISO plants with multiple operating points and with parametric and unstructured uncertainties. *International Journal of Control*, 75(4):219–241, April 2002.
- [Zuo, 2010] Z. Zuo. Trajectory tracking control design with command-filtered compensation for a quadrotor. *IET Control Theory and Application*, 4(11):2343–2355, January 2010.